Inorg. Chem. **2002**, *41*, 2941–2945

Density Functional Theory Calculations of Selected Ru(II) Two Ring Diimine Complex Dications

Stanislav R. Stoyanov, John M. Villegas, and D. P. Rillema*

Department of Chemistry, Wichita State University, Wichita, Kansas 67260-0051

Received October 15, 2001

Geometry optimization for a series of ten, two-ring diimine Ru(II) complexes was effected using the Gaussian 98 protocol at density functional theory (DFT) B3LYP level with basis sets 3-21G(*) and 3-21G(*)(*). HOMO–LUMO energy difference values compared favorably to the experimental data from electrochemistry [$\Delta E_{1/2} = (E_{1/2ox} - E_{1/2red})$] and the lowest energy absorption maxima, which for these complexes correspond to the metal-to-ligand charge transfer (MLCT) band. The HOMO and LUMO distributions from DFT support the idea that the lowest energy transitions are metal-to-ligand charge transfer and that the lowest energy LUMO for the mixed ligand complexes is located on 2,2′-bipyrazine (bpz), followed by 2,2′-bipyrimidine (bpm) and then 2,2′-bipyridine (bpy).

Introduction

An extensive number of publications have appeared during the last three decades on excited-state processes[1−3] occurring between transition metals and coordinated nitrogen containing heterocycles. The physical and photophysical properties of these complexes related to metal-to-ligand charge transfer have been extensively studied by UV−vis absorption and emission spectroscopy and by electrochemical investigations.[4−8] Because they are robust and exhibit strong emission and photoinduced electron transfer, Ru(II) polypyridyl complexes[9,10] have been a special area of research for the development of sensors and photosensitizers. One device of particular interest has been the Grätzel cell: a solar energy regenerative apparatus useful for conversion of solar energy[3] into electricity. Of specific interest in these developments has been the model compound, $[Ru(bpy)_3]^{2+}$, with its long emission lifetime and unique luminescent properties.[9−12] Consequently, its properties have been the subject of detailed characterizations including its crystal structure[13,14] and chiral recognition.[15]

In addition to the experimental studies, Ru(II) polypyridine complexes have been very attractive to theoretical chemists.[16−22] Various methods have been used in attempts to correlate experimental findings with theoretical predictions. Reports have appeared describing CNDO/CI,[16] INDO/CI,[17,19,21,22] and ZINDO[23] semiempirical calculations on electronic spectra and geometries of Ru(II) diimine complexes. The CI method was employed using canonical molecular orbitals for dinuclear systems.[20] PM3 and ab initio

* To whom correspondence should be addressed. E-mail: paul.rillema@wichita.edu.

(1) Wrighton, M. *J. Chem. Educ*. **1983**, *60*, 877.
(2) Scandola, F. *J. Chem. Educ*. **1983**, *60*, 814.
(3) Kutal, C. *J. Chem. Educ*. **1983**, *60*, 882.
(4) Ross, H. P.; Boldaji, M.; Rillema, D. P.; Blanton, C. B.; White, R. P. *Inorg. Chem*. **1989**, *28*, 1013.
(5) Haarmann K. Master Thesis, University Fribourg, 1986.
(6) Rillema, D. P.; Allen, G.; Meyer, T. J.; Conrad, D. *Inorg. Chem*. **1983**, *22*, 1617.
(7) Curtis, J. C.; Sullivan, B. P.; Meyer, T. J. *Inorg. Chem*. **1983**, *22*, 224.
(8) Kawanishi, Y.; Kitamura, N.; Kim, Y.; Tazuke, S. *Sci. Pap. Inst. Phys. Chem. Res. (Jpn.)* **1984**, *78*, 212−219.
(9) Watts, R. *J. Chem. Educ*. **1983**, *60*, 834.
(10) Juris, A.; Balzani, V.; Barigelletti, F.; Campagna, S.; Belser, P.; von Zelewski, A. *Coord. Chem. Rev*. **1988**, *84*, 85.
(11) Klassen, D. M.; Crosby, G. A. *J. Chem Phys*. **1965**, *43*, 1498.
(12) Lytle, F. E.; Hercules, D. M. *J. Am. Chem. Soc*. **1969**, *91*, 23.
(13) Rillema, D. P.; Jones, D. S.; Woods, C.; Levy, H. A. *Inorg. Chem*. **1992**, *31*, 31.
(14) Lai, H.; Jones, D. S.; Schwind, D. C.; Rillema, D. P. *J. Crystallogr. Spectrosc. Res*. **1990**, *20*, 321−5.
(15) Breu, J.; Domel, H.; Stoll, A. *Eur. J. Inorg Chem*. **2000**, *11*, 2401−2408.
(16) Ivanova, N. V.; Sizov, O. V.; Nikolskii, A. B.; Panin, A. I. *J. Struct. Chem*. **1999**, *40*, 620−23.
(17) Sizova, O. V.; Panin, A. I.; Ivanova, N. V.; Baranovskii, V. I. *J. Struct. Chem*. **1997**, *38*, 366−74.
(18) Sizova, O. V.; Baranovskii, V. I.; Ivanova, N. V.; Panin, A. I. *J. Struct. Chem*. **1997**, *38*, 183−93.
(19) Sizova, O. V.; Baranovskii, V. I.; Ivanova, N. V.; Panin, A. I. *J. Struct. Chem*. **1996**, *37*, 206−19.
(20) Sizova, O. V.; Baranovskii, V. I.; Ivanova, N. V.; Panin, A. I. *Russ. J. Coord. Chem*. **1997**, *23*, 256−65.
(21) Sizova, O. V.; Baranovskii, V. I.; Ivanova, N. V.; Panin, A. I. *Russ. J. Coord. Chem*. **1996**, *22*, 556−62.
(22) Sizova, O. V.; Baranovskii, V. I..; Ivanova, N. V.; Panin, A. I. *Russ. J. Coord. Chem*. **1997**, *23*, 256−65.
(23) Gorelsky, S. I.; Dodsworth, E. S.; Lever, A. B. P.; Vlcek, A. A. *Coord. Chem. Rev*. **1998**, *174*, 469−494.

10.1021/ic0110629 CCC: $22.00
Published on Web 05/10/2002

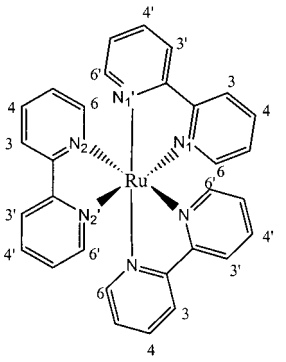

Figure 1. Schematic diagram of the complexes studied.

studies have been reported on the relative stability of cis and trans complexes of Ru(II) containing 1,10-phenanthroline as the ligand.[24]

More recently, calculations based on DFT have appeared in the literature. Some examples of the utility of these calculations follow: Calculations on ligand substituent effects[25] in $[Ru(bpy)_2(R_2bpy)]^{2+}$ complexes have been reported, where R = methoxy or nitro located at the 4,4′-positions. The ^{17}O chemical shielding[26] in d^0 transition metal oxo complexes, including RuO_4, have been presented and analyzed. Geometry optimization and excited-state calculations of $[Ru(bpy)_3]^{2+}$ at the DFT level have been discussed.[27] Finally, electronic transitions of $[Ru(bpy)_3]^{2+}$ in D_3 symmetry have been studied by DFT,[28] and a symmetry based electronic spectrum interpretation has been provided.

In this publication, the HOMO−LUMO energy difference in $[Ru(bpy)_3]^{2+}$ and nine related complexes (for notation, see Figure 1) has been theoretically investigated using DFT/B3LYP protocols and found to correlate well with $\Delta E_{1/2}$ [$\Delta E_{1/2} = (E_{1/2ox} - E_{1/2red})$] from cyclic voltammetry and with the lowest energy transition from the UV−vis spectrum previously assigned as metal-to-ligand charge transfer (MLCT). We also show that plots of the energy of the LUMO versus $E_{1/2}^{red}$ and of the energy of the HOMO versus $E_{1/2}^{ox}$ support the fact that the easier to reduce complexes have lower lying LUMOs and those that are easier to oxidize have higher energy HOMOs. In addition, the HOMO and LUMO frontier orbitals are shown to be consistent with the MLCT interpretation.

Experimental Section

Calculations were effected using Gaussian 98W, version 5.4 (Rev. A9), and Gaussian 98 for UNIX, Rev A9. The Gaussian Job Files were imported into Gaussian 98W from PDB format of PC Spartan Pro, version 1.0.1. Files were viewed in GaussViewW, Rev. 2.1. Gaussian 98W was run on a PC Pentium III platform, and Gaussian 98 for UNIX was run on the supercomputer located in the High Performance Computing Center at WSU.

Theoretical Section

It is well-known that the electron correlation is very important for heterocycles that have more than one heteroatom per ring[29] and for transition metal complexes.[30] The motion of an electron is actually governed not by the average positions of the other electrons, but by their instantaneous positions. Thus, the electron motion is in fact correlated to that of all the other electrons. The Hohenberg−Kohn theorem, which is the basis of the density functional theory, states that the minimal energy of a collection of electrons under the influence of an external field is a functional (a function of a function) of the electron density.[30] In DFT, instead of the exact exchange for a single determinant, a more general expression, the exchange−correlation functional, is used which can include terms for both the exchange energy and the electron correlation. The general DFT equation is $E_{KS} = V + \langle hP \rangle + {}^1/_2\langle PJ(P) \rangle + E_X[P] + E_C[P]$, where V is the nuclear repulsion energy, P is the density matrix, $\langle hP \rangle$ is the one-electron (kinetic plus potential) energy, ${}^1/_2\langle PJ(P) \rangle$ is the classical Coulombic repulsion of the electrons, $E_X[P]$ is the exchange functional, and $E_C[P]$ is the correlation potential.[31] The calculations here utilize Becke's 3 parameter hybrid method (B3) for the calculation of the exchange−correlation energy containing the Lee, Yang, and Parr (LYP)[32] nonlocal correlation functional according to the equation $E_{XC} = (A \times E_X^{Slater}) + [(1 - A) \times E_X^{Hartree-Fock}] + (B \times \Delta E_X^{Becke}) + E_C^{VWN} + (C \times E_C^{LYP})$, where A, B, and C are the constants determined by Becke for fitting of the energy equation to the Gaussian 1-G1 molecule set,[33] VWN is Vosko, Wilk, and Nussair 1980 correlation functional, referred to as local spin density (LSD) correlation.[34]

For the DFT calculations, a mathematical representation of the molecular orbitals within the molecule or basis set is specified. The basis set is like restricting an electron to a particular region of space, and consequently, larger basis sets mean fewer constraints on electrons. Larger basis sets result in a more accurate approximation of the molecular orbital. The restriction on the basis set of choice in this study is imposed by the Ru atom, 3-21G$^{(*)(*)}$,[35−37] which is the largest standard basis set in Gaussian 98 that can be used for it. Mixed basis set calculations using 6-311G$^{(*)}$[38,39] for N, C, and H atoms and 3-21G$^{(*)}$ for Ru only were also attempted in order to improve the molecular structure and the energy fitting. The last scheme was applied for B3LYP calculations only.

Results and Discussion

As noted by the data in Table 1, the DFT method gave structural values in relatively good agreement with those

(24) Concepcion, J.; Loeb, B.; Simon-Manso, Y.; Zuloaga, F. *Polyhedron* **2000**, *19*, 2297−2302.
(25) Zheng, K.-C.; Kuang, D.-B.; Sheng, Y.; Wang, J.-P. *Wuli Huaxue Xuebao* **2001**, *17*, 43−47.
(26) Kaupp, M.; Malkina, O.; Malkin, V. *J. Chem. Phys.* **1997**, *106*, 9201−9212.
(27) Buchs, M.; Daul, C. *Chimia* **1998**, *52*, 163−166.
(28) Daul, C.; Baerends, E. J.; Vernooijs, P. *Inorg. Chem.* **1994**, *33*, 3538−3543.
(29) Davarski, K. A.; Halachev, H. K.; Yankova, R. Z.; Stoyanov, S. *Chem. Heterocycl. Compd. (Chichester, U.K.)* **1998**, *5*, 645−651.
(30) *Titan Tutorial and User's Guide*; WaveFunction, Inc.: Irvine, CA, 2000.
(31) Frisch, W. J.; Frisch, Æ.; Foresman, J. B. *Gaussian 94 User's Reference*; Gaussian Inc.: Pittsburgh, PA, 1994−1995.
(32) Lee, C.; Yang, W.; Parr, R. G. *Phys. Rev.* **1988**, *B37*, 785−789.
(33) Becke, A. D. *J. Chem. Phys.* **1993**, *98*, 5648−5652.
(34) Vosko, S. H.; Wilk, L.; Nusair, M. *Can. J. Phys.* **1980**, *58*, 1200−1211.
(35) Binkley, J. S.; Pople, J. A.; Hehre, W. J. *J. Am. Chem. Soc.* **1980**, *102*, 939.
(36) Gordon, M. S.; Binkley, J. S.; Pople, J. A.; Pietro, W. J.; Hehre, W. J. *J. Am. Chem. Soc.* **1982**, *104*, 2797.
(37) Pietro, W. J.; Francl, M. M.; Hehre, W. J.; Defrees, D. J.; Pople, J. A.; Binkley, J. S. *J. Am. Chem. Soc.* **1982**, *104*, 5039.
(38) McLean, A. D.; Chandler, G. S. *J. Chem. Phys.* **1980**, *72*, 5639.
(39) Krishnan, R.; Binkley, J. S.; Seeger, R.; Pople, J. A. *J. Chem. Phys.* **1980**, *72*, 650.

Table 1. Selected Geometry Parameters for Ru(II) Tris Complexes Taken Form X-ray Crystallography[13,14] and from DFT Calculations

Bond Lengths (Å)

	experimental (PF_6 salts)			DFT/3-21G*		
bond	$[Ru(y)_3]^{2+}$	$[Ru(m)_3]^{2+}$	$[Ru(z)_3]^{2+}$	$[Ru(y)_3]^{2+}$	$[Ru(m)_3]^{2+}$	$[Ru(z)_3]^{2+}$
Ru−N*[a]	2.056(2)	2.067(4)	2.05(1)	2.1053	2.1051	2.1047
C[b]−N*−	1.354(4)	1.351(4)	1.37(2)	1.3588	1.3611	1.3578
C[b]−N[c]		1.341(4)	1.33(2)		1.3508	1.3578
C[b]−C−	1.369(4)	1.369(4)	1.40(4)	1.3969	1.3919	1.3926
>C−N−[d]	1.354(3)	1.355(4)	1.33(3)	1.3724	1.3716	1.3727
>C−N[c]		1.321(4)			1.3308	
>C−C−	1.369(4)		1.42(3)	1.397		1.4
>C−C<	1.474(5)	1.481(4)	1.48(4)	1.4721	1.4721	1.4607

Selected Bond Angles (deg)

	experimental (PF_6 salts)			DFT/3-21G**		
angle	$[Ru(y)_3]^{2+}$	$[Ru(m)_3]^{2+}$	$[Ru(z)_3]^{2+}$	$[Ru(y)_3]^{2+}$	$[Ru(m)_3]^{2+}$	$[Ru(z)_3]^{2+}$
N1−Ru−N2′	173.0(1)	172(2)	172.3(4)	173.33	173.56	173.436
C(6′)−N−C<	118.0(2)	116.3(4)	118(2)	119.1	117.15	118.221
C−Nb−C		116.1(3)	118(2)		118.19	117.559
C−C−C	119.6(5)	118.0(3)		118.95	117.8	
N−Ru−N	78.7(1)	78.3(3)	78.6(4)	78.137	78.41	78.3705
N1′−Ru−N2	89.1(1)	90(2)	90(2)	88.217	88.24	88.1791
N1′−Ru−N2′	96.3(1)	96(2)	96(1)	96.9	97.06	96.9403

[a] Asterisk indicates N bonding to Ru. [b] (Ring) −C−. [c] N nonbonding to Ru. [d] > indicates bridging C.

determined by X-ray diffraction for $[Ru(bpy)_3](PF_6)_2$, $[Ru(bpm)_3](PF_6)_2$, and $[Ru(bpz)_3](PF_6)_2$, where bpm = 2,2′-bipyrimidine, bpy = 2,2′-bipyridine, and bpz = 2,2′-bipyrazine. The Ru−N bond length calculated using the DFT/B3LYP method with the 3-21G* basis set was by ∼0.04 Å longer in comparison to the X-ray determined value. The other bond lengths, however, were very well reproduced. The DFT nonlocal corrections using Becke[40] exchange and Perdew[41] correlation functionals (generalized gradient approximation (GGA)) produced a Ru−N bond length[22] of 2.099 Å, which is very close to our result. The DFT calculated values for the bond angles were in closest agreement. The highest deviation was about 2° for the [C−N(nonbonding)−C] bond angle in $[Ru(bpm)_3]^{2+}$.

The energies of the frontier molecular orbitals form the DFT/B3LYP calculation for the series of 10 diimine complexes of Ru(II) are plotted in Figure 2, arranged by ascending LUMO energies. The energy differences between the HOMO and HOMO(−1) orbitals ranged from 0.1570 to 0.2005 eV, and those between LUMO and LUMO(−1) ranged from 0.0911 to 0.3864 eV. The lowest lying set of frontier orbitals belonged to $[Ru(bpz)_3]^{2+}$, intermediate to $[Ru(bpm)_3]^{2+}$, and the highest to $[Ru(bpy)_3]^{2+}$. The mixed ligand complexes fell into the same order with the LUMO localized on the bpz ligand as lowest in energy, then bpm, and finally bpy at the highest energy. This trend parallels the reduction properties of these complexes which fell into the series bpz > bpm > bpy.[42]

Experimental $\Delta E_{1/2}$ values [$\Delta E_{1/2} = (E_{1/2ox} - E_{1/2red})$] and MLCT band energies and DFT calculated LUMO and HOMO energies are presented in Table 2. All the $\Delta E_{1/2}$ values (vs SCE) and electronic transitions were determined in CH_3CN. To analyze the ability of the DFT method to reproduce the experimental results for the series of complexes, a plot of the calculated LUMO−HOMO energy difference versus the lowest energy transition (MLCT band)

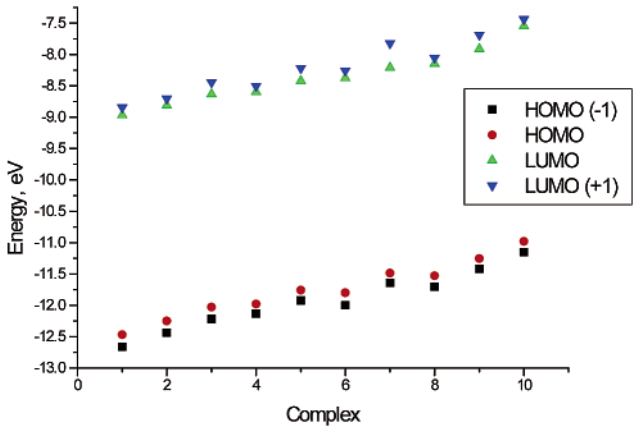

Figure 2. Plot of the distribution of frontier molecular orbital energies calculated using DFT/B3LYP/3-21G(*). The numbers on the *x*-axis correspond: 1 = $Ru(z)_3$, 2 = $Ru(z)_2(m)$, 3 = $Ru(z)(m)_2$, 4 = $Ru(z)_2(y)$, 5 = Ru(y)(m)(z), 6 = $Ru(m)_3$, 7 = $Ru(z)(y)_2$, 8 = $Ru(m)_2(y)$, 9 = Ru((m)$(y)_2$, and 10 = $Ru(y)_3$.

Table 2. Experimental $\Delta E_{1/2}$ [$\Delta E_{1/2} = (E_{1/2ox} - E_{1/2red})$] (V vs SCE), Experimental MLCT Band Energies (eV), and LUMO−HOMO Energy Differences (eV) from DFT-B3LYP/3-21G* Calculations, L-H (DFT)

complex	L-H(DFT)	$\Delta E_{1/2}$	MLCT band
$[Ru(y)_2z]^{2+}$ [4]	3.2757	2.40	2.62
$[Ru(y)_2m]^{2+}$ [4,43]	3.3416	2.42	2.58
$[Ruymz]^{2+}$ [4]	3.3331	2.49	2.67
$[Ruy(m)2]^{2+}$ [6,7]	3.3832	2.50	2.69
$[Ruy(z)_2]^{2+}$ [6,7]	3.3829	2.51	2.67
$[Ru(m)_2z]^{2+}$ [4]	3.3913	2.57	2.74
$[Ru(y)_3]^{2+}$ [4]	3.4308	2.58	2.75
$[Ru(m)_3]^{2+}$ [4]	3.4237	2.60	2.73
$[Ru(z)_2m]^{2+}$ [4]	3.4537	2.62	2.76
$[Ru(z)_3]^{2+}$ [4]	3.5016	2.66	2.82

(40) Becke, A. D. *Phys. Rev. A: At., Mol., Opt., Phys.* **1988**, *38*, 3098.
(41) Perdew, J. P. *Phys. Rev. B: Condens. Matter.* **1986**, *33*, 8822.
(42) Dose, E. V.; Wilson, L. J. *Inorg. Chem.* **1978**, *17*, 2660.
(43) D'Angelantonio, M.; Mulazzani, Q. G.; Venturi, M.; Ciano, M.; Hoffman, M. Z. *J. Phys. Chem.* **1991**, *95*, 5121−5129.

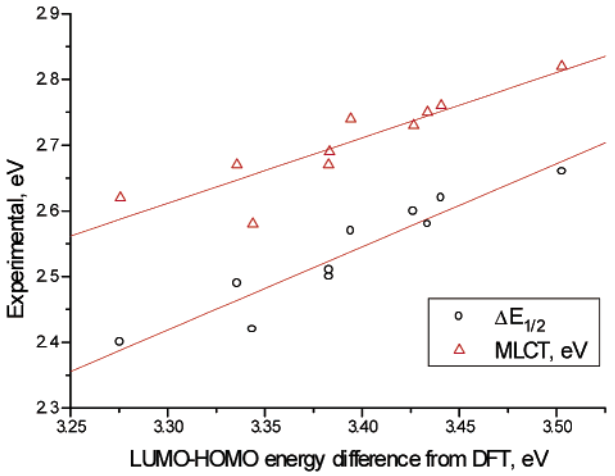

Figure 3. Plot of the DFT calculated LUMO−HOMO energy differences vs $\Delta E_{1/2}$ and MLCT band energies for the 10 complexes.

and $\Delta E_{1/2}$ is presented in Figure 3. The experimental values therefore can be predicted from the DFT calculated energy gap using the slope and the intercept from the linear regression analysis. For $\Delta E_{1/2}$ versus the LUMO−HOMO energy difference, a slope of 1.26 and an intercept of −1.76 (R^2 = 0.90) are obtained. For the MLCT band versus the LUMO−HOMO energy difference, a correlation coefficient (R^2) of 0.8, a slope of 1.00, and an intercept of 0.67 were obtained.

For all 10 complexes, a plot of $E_{1/2}^{red}$ versus the LUMO energy is presented in Figure 4a, and a plot of $E_{1/2}^{ox}$ versus the HOMO energy is presented in Figure 4b. The slope of the line in Figure 4a is 2.321 with a correlation coefficient of R^2 =0.937; the slope of the line in Figure 4b is 2.091 with a correlation coefficient of R^2 = 0.994. These correlations are impressive.

The spatial distributions of the frontier orbitals for $[Ru(bpy)_3]^{2+}$ and $[Ru(bpy)(bpz)_2]^{2+}$ calculated using DFT/B3LYP/3-21G* are shown in Figure 5. For the DFT calculated orbitals, the HOMOs are mostly located on the metal atom showing a clear d_{z^2} shape whereas the LUMOs are located on the ligands. For $[Ru(bpy)_3]^{2+}$, the LUMO is spread equally over the three bpy ligands consistent with D_3 symmetry; for $[Ru(bpy)(bpz)_2]^{2+}$, the LUMO is localized over the two bpz ligands consistent with their electrochemical assignment as being the most reducible of the ligands. The DFT calculations result in HOMOs and LUMOs consistent with the lowest energy transition assigned as MLCT. On the basis of Figures 2−5, and Table 2, it can be concluded that DFT/B3LYP calculations result in close agreement with the experimental measurements describing the lowest energy transition in all selected complexes in accordance with the MLCT model.

No improvement in the data fitting was observed for the 3-21G(*)(*) basis set compared to the 3-21G(*) basis set for the DFT calculations. The changes in the HOMO−LUMO energy difference and in the geometry parameters were in the thousandth or less. Mixed basis set calculation (using 3-21G(*) on Ru atom and 6-311G(*) on N, C, and H atoms) for $[Ru(bpy)_3]^{2+}$ yielded Ru−N bond lengths by ∼0.005 Å

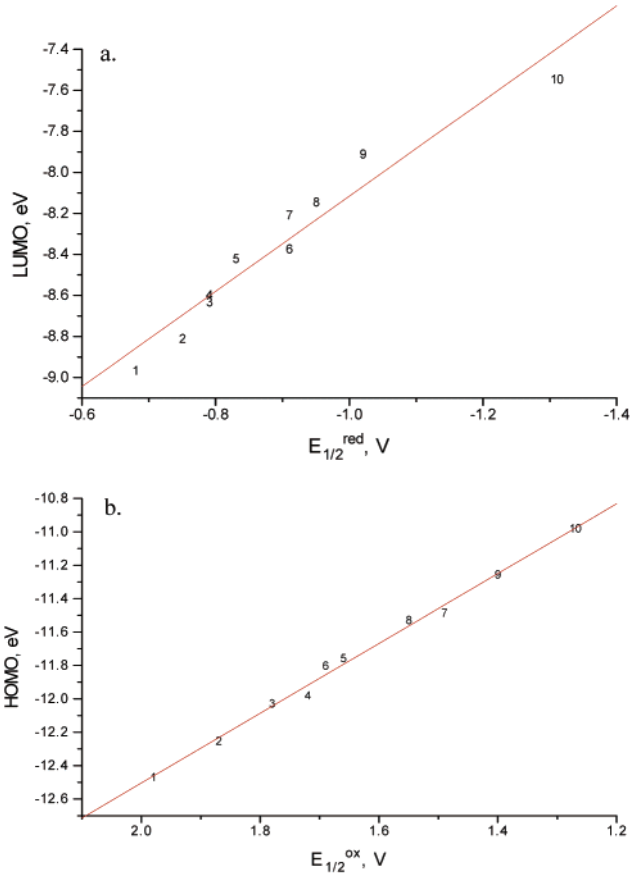

Figure 4. Plot of (a) $E_{1/2}^{red}$ (V vs SCE) vs LUMO energies (eV) and (b) $E_{1/2}^{ox}$ (V vs SCE) vs HOMO energies (eV) calculated using DFT/B3LYP/3-21G(*). 1 = $Ru(z)_3$, 2 = $Ru(z)_2(m)$, 3 = $Ru(z)(m)_2$, 4 = $Ru(z)_2(y)$, 5 = Ru(y)(m)(z), 6 = $Ru(m)_3$, 7 = $Ru(z)(y)_2$, 8 = $Ru(m)_2(y)$, 9 = $Ru(m)(y)_2$, and 10 = $Ru(y)_3$.

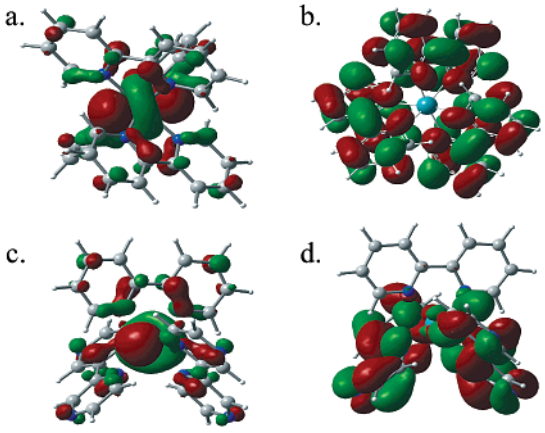

Figure 5. HOMOs and LUMOs for two complex dications from DFT/B3LYP calculations: (a) HOMO of $[Ru(y)_3]^{2+}$, (b) LUMO of $[Ru(y)_3]^{2+}$, (c) HOMO of $[Ruy(z)_2]^{2+}$, (d) LUMO of $[Ruy(z)_2]^{2+}$.

longer than the ones from 3 to 21G(*) calculations, hence, less accurate than the latter. The convergence difficulties encountered and the high cost of the calculations appeared counterproductive for using the mixed basis set.

Work on the singlet and triplet energy transitions in these and other Ru complexes with the TD-DFT routine of Gaussian program package is now in progress.

Conclusion

Full geometry optimization was effected on ten Ru(II) two-ring diimine complexes using DFT-B3LYP/3-21G$^{(*)}$ and DFT-B3LYP/3-21G$^{(*)(*)}$ theoretical methods. The results from DFT calculations were in good agreement with the X-ray crystallography structures for three of the complexes. HOMO−LUMO energy differences were plotted versus the experimental $\Delta E_{1/2}$ values and MLCT energies. Plots of the frontier orbital distributions demonstrated the similarity in the electronic energy distribution within the group of 10 complexes. The HOMO was basically localized on the metal center, and the LUMO was located on the most reducible ligand(s). The spatial distributions are consistent with assigning the lowest energy electronic transitions as MLCT in these types of complexes.

Acknowledgment. The authors thank Dr. M. Zandler for his many helpful discussions and the Wichita State University High Performance Computing Center, the Kansas NSF Cooperative Agreement EPS-9874732, and the Department of Energy for support.

IC0110629